Supplement of Biogeosciences, 22, 6727–6748, 2025
https://doi.org/10.5194/bg-22-6727-2025-supplement

Biogeosciences
Open Access

Supplement of

Reduction of carbon, alkalinity and nutrient fluxes in the southern Baltic Sea caused by dragging of otter trawl nets across the seafloor

Pankan Linsy et al.

Correspondence to: Pankan Linsy (linsyp@geomar.de)

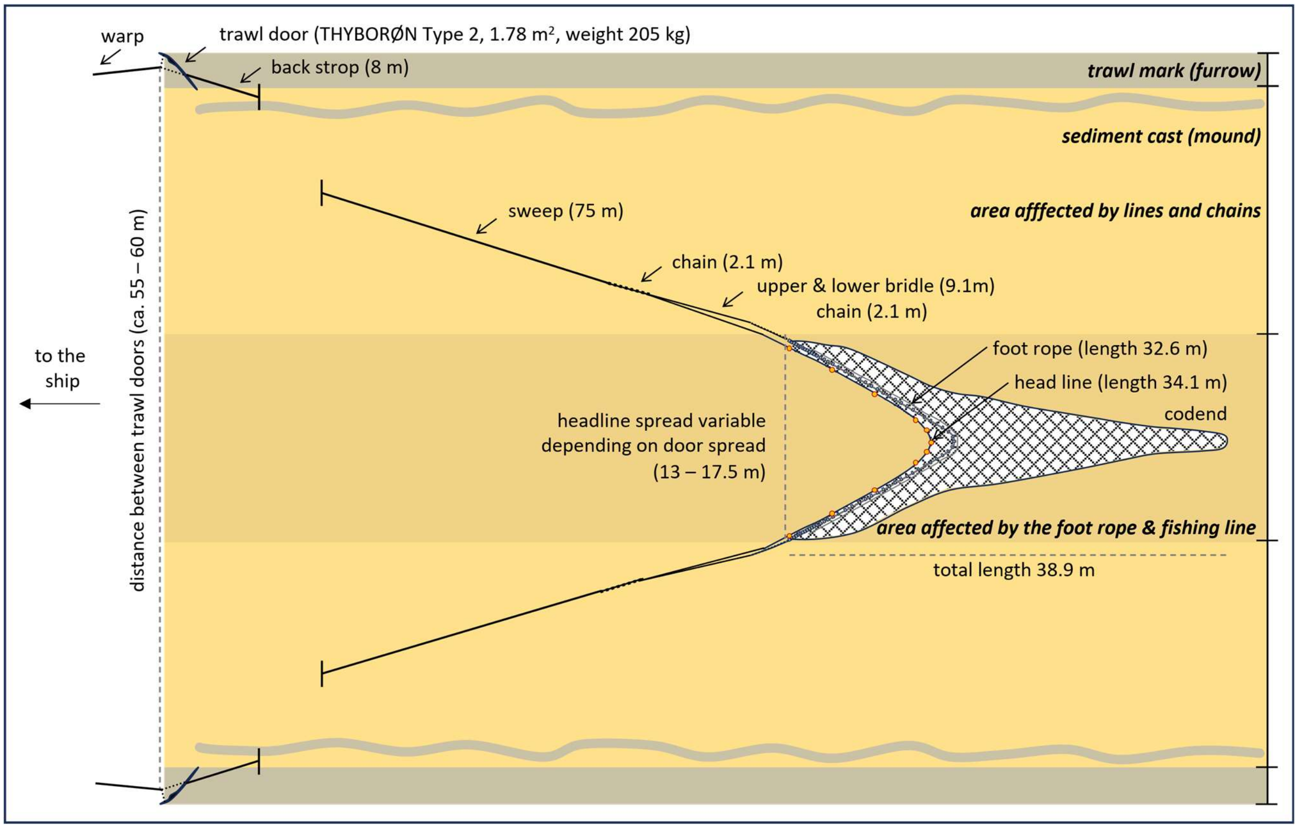

Figure S1. Schematic of the otter trawl (TV-3#520×80 mesh) used for the trawling experiment. The gear was fitted with Thyborøn Type 2 Standard trawl doors (surface area: 1.78 m² each). The distance between the otter boards was approximately 55–60 m (ICES, 2017). Shaded areas indicate sediment disturbance by different components.

Table S1: Station list of the multiple cores (MUC), benthic landers (BIGO), CTD, and DSR deployments.

Station	Gear number	Date (2024)	Latitude	Longitude	Location
1	CTD-1	19 Jul	54° 12.137' N	11° 42.341' E	North of HI
4	MUC-1*	19 Jul	54° 11.944' N	11° 42.568' E	HI (=CL)
5	MUC-2*	19 Jul	54° 11.925' N	11° 42.160' E	HI (=CL)
7	CTD-2	19 Jul	54° 11.990' N	11° 42.236' E	HI
12	MUC-5	20 Jul	54° 12.029' N	11° 42.144' E	HI
13	BIGO-1-1	20 Jul	54° 12.006' N	11° 42.501' E	HI
14	MUC-6	21 Jul	54° 12.026' N	11° 42.364' E	HI
15	MUC-7	21 Jul	54° 11.945' N	11° 41.216' E	CL
17	BIGO-2-1	21 Jul	54° 12.043' N	11° 41.958' E	HI
18	DSR-1	21-23 Jul	54° 11.958' N	11° 42.319' E	HI
20	MUC-9	22 Jul	54° 11.932' N	11° 42.582' E	HI
28	MUC-12	25 Jul	54° 12.062' N	11° 41.252' E	CL
29	BIGO-2-2	25 Jul	54° 12.056' N	11° 41.104' E	CL
30	DSR-2	25 - 27 Jul	54° 11.979' N	11° 41.376' E	CL
31	CTD-3	26 Jul	54° 12.050' N	11° 41.240' E	CL
34	BIGO-1-2	26 Jul	54° 11.961' N	11° 42.377' E	HI
37	MUC-15	27 Jul	54° 12.022' N	11° 42.172' E	HI
45	MUC-20	28 Jul	54° 11.934' N	11° 41.230' E	CL
46	DSR-3	28-30 Jul	54° 11.935' N	11° 42.340' E	HI
47	CTD-4	29 Jul	54° 11.938' N	11° 42.315' E	HI
48	MUC-21	29 Jul	54° 11.934' N	11° 42.575' E	HI
49	MUC-22	29 Jul	54° 12.018' N	11° 42.366' E	HI
50	BIGO-1-3	29 Jul	54° 12.016' N	11° 42.323' E	HI
52	MUC-23	30 Jul	54° 11.948' N	11° 41.212' E	CL
53	BIGO-2-3	30 Jul	54° 12.040' N	11° 41.037' E	CL
55	DSR-4	30 Jul - 2 Aug	54° 11.935' N	11° 41.029' E	CL
60	BIGO-1-4	31 Jul	54° 12.025' N	11° 42.672' E	HI
62	MUC-26	1 Aug	54° 12.036' N	11° 41.220' E	CL
64	CTD-5	1 Aug	54° 11.964' N	11° 42.177' E	HI
65	CTD-6	1 Aug	54° 11.999' N	11° 41.243' E	CL
69	MUC-28	3 Aug	54° 12.025' N	11° 42.101' E	HI
70	MUC-29	3 Aug	54° 12.039' N	11° 42.345' E	HI
72	BIGO-1-5	3 Aug	54° 11.964' N	11° 42.330' E	HI
73	DSR-5	3 - 5 Aug	54° 11.984' N	11° 42.102' E	HI
75	CTD-7	4 Aug	54° 11.943' N	11° 41.230' E	CL
76	MUC-31	4 Aug	54° 11.949' N	11° 41.225' E	CL
78	MUC-33	4 Aug	54° 11.942' N	11° 42.594' E	HI
79	BIGO-2-4	4 Aug	54° 11.930' N	11° 41.199' E	CL
84	DSR-6	5 - 8 Aug	54° 12.025' N	11° 42.435' E	HI
85	BIGO1-6	5 Aug	54° 12.025' N	11° 42.615' E	HI

*Note: Data from MUC1 and MUC2 were collected prior to disturbance and are considered as controls.

Table S2: Mean and standard deviation of particulate concentrations at the study site. Bolded numbers indicate statistically significant differences (*p<0.05) between the control (CL) and High Impact (HI) sites.

Depth (cm)		0.5	1.5	2.5	3.5	4.5	5.5	7	9	11	13	16	20	24	28	31
POC wt.%	CL	***3.58±0.74**	***3.4±0.71**	3.05±0.7	2.83±0.48	2.83±0.43	2.79±0.32	2.55±0.5	2.04±0.45	1.72±0.42	1.45±0.16	1.61±0.49	1.87±0.45	2.14±0.25	1.96±0.17	1.67±0.3
	HI	***2.77±0.78**	***2.44±0.99**	2.78±0.66	2.96±0.7	2.85±0.93	2.69±0.54	2.13±0.47	1.87±0.54	1.71±0.52	1.44±0.36	1.92±0.41	1.9±0.54	2.03±0.22		
PON wt.%	CL	***0.54±0.11**	***0.5±0.12**	0.44±0.11	0.4±0.08	0.4±0.06	0.39±0.05	0.35±0.07	0.27±0.06	0.22±0.05	0.19±0.01	0.21±0.06	0.23±0.05	0.27±0.03	0.25±0.02	0.22±0.04
	HI	***0.41±0.12**	***0.35±0.15**	0.4±0.1	0.41±0.11	0.43±0.13	0.38±0.08	0.29±0.08	0.25±0.08	0.23±0.07	0.19±0.05	0.24±0.06	0.24±0.07	0.26±0.03		
C/N	CL	7.75±0.26	7.89±0.29	8.16±0.3	8.24±0.48	8.18±0.26	8.34±0.15	8.62±0.41	8.93±0.25	9.21±0.65	9.11±0.55	9.07±0.69	9.28±0.54	9.19±0.22	9.2±0.51	8.7±0.01
	HI	7.93±0.38	8.2±0.53	8.06±0.49	8.44±0.61	8.47±0.76	8.39±0.55	8.59±0.69	8.87±0.66	8.9±0.48	8.73±0.75	9.21±0.62	9.46±0.99	9.33±0.65		
CaCO3 wt.%	CL	***5.39±1.12**	***4.87±1.88**	3.43±1.76	2.65±1.19	2.7±0.87	2.56±0.41	2.38±0.83	1.73±0.52	1.25±0.54	1±0.64	1.14±0.67	1.1±0.76	1.79±0.58	1.61±0.71	2.34±0.33
	HI	***3.55±0.48**	***2.77±1.56**	3.5±1.13	2.65±1.76	2.84±2.49	3.17±3.03	1.86±0.94	1.35±0.8	1.21±0.67	1.05±0.39	1.4±0.64	1.35±0.57	1.54±0.42		
TS wt.%	CL	0.62±0.13	0.55±0.1	0.54±0.1	0.62±0.14	0.71±0.13	0.8±0.09	0.85±0.08	0.76±0.08	0.75±0.1	0.83±0.2	0.99±0.3	0.89±0.17	1.02±0.16	1.02±0.07	0.86±0.1
	HI	0.49±0.17	0.42±0.22	0.55±0.14	0.75±0.23	0.81±0.3	0.79±0.17	0.66±0.13	0.66±0.15	0.77±0.16	0.88±0.25	1.03±0.11	0.9±0.27	0.98±0.1		

Table S3: Mean and standard deviation of porewater solute concentrations at the study site. Bolded numbers indicate statistically significant differences between the control (CL) and High Impact (HI) sites.

Depth (cm)		0	0.5	1.5	2.5	3.5	4.5	5.5	7	9	11	13	16	20	24
TA (mM)	CL	2.17±0.04	2.86±0.23	3.23±0.41	3.28±0.39	3.38±0.45	3.68±0.52	3.95±0.49	4.28±0.34	4.6±0.3	4.94±0.24	5.16±0.26	5.39±0.24	5.64±0.29	5.78±0.37
	HI	2.18±0.07	2.69±0.27	2.94±0.4	2.95±0.36	3.08±0.38	3.35±0.38	3.56±0.39	3.91±0.48	4.31±0.65	4.77±0.91	5.12±0.94	5.5±1.21	5.9±1.11	6.55±0.89
NH_4^+ (µM)	CL	6.3±4.6	78±25	128±42	149±42	159±49	189±49	201±45	226±38	247±40	273±34	273±32	299±32	314±34	321±44
	HI	6.1±2.7	59±26	95±37	122±43	131±73	159±45	185±49	218±54	236±69	284±99	286±83	328±91	372±104	415±67
PO_4^{3-} (µM)	CL	1.2±0.3	55±45	89±36	64±23	54±20	57±20	61±20	65±16	70±14	72±13	71±14	69±12	71±11	71±12
	HI	1.1±0.3	55±62	62±63	52±28	43±16	46±12	45±8	52±8	61±12	64±15	70±16	74±17	80±20	84±18
NO_3^-(µM)	CL	6.9±1.5	0.95±1	1.27±1.16	1.12±1.35	1.21±1.29	1.06±1.27	0.85±0.69	1.6±0.27						
	HI	5.8±0.7	0.39±0.28	0.63±0.5	0.88±0.58	1.08±0.88	0.47±0.41	0.33±0.21	0.6±0.4						
NO_2^-(µM)	CL	0.24±0.01	0.93±0.45	1.34±0.43	0.61±0.3	0.3±0.21	0.24±0.17	0.29±0.22	0.28±0.19						
	HI	0.2±0.08	0.73±0.7	0.8±0.46	0.39±0.3	0.18±0.24	0.22±0.24	0.23±0.29	0.27±0.3						
H_2S (µM)	CL	0.38±0.1	5.7±2.9	4.2±2.1	5.8±1.9	8.4±2.6	14.3±3.1	29.3±8.6	47.6±17.1	74.4±29	95.5±41.8	112±56.3	129±69	144±64	169±73
	HI	0.31±0.09	4.5±2.1	4.2±0.3	5.4±1.5	8.6±4.2	16.2±8.5	32.8±20.6	57.5±28.7	86.6±61	118±75	144±98	157±103	182±116	202±131
Fe^{2+} (µM)	CL	0.43±0.14	136±77.8	169.9±59.3	91.7±55.7	24.4±27	4.7±4.2	1.3±0.8	1.3±0.7	1.3±0.8	1.2±0.5	1±0.3	0.9±0.4	0.8±0.4	0.9±0.5
	HI	0.59±0.22	90.5±90.4	128.9±59.3	70.2±51	14.7±17.6	7.7±9.3	1.5±1.1	1.2±0.3	1.8±1.1	1.4±0.5	1.1±0.5	0.9±0.5	0.9±0.4	1.1±0.4
$Si(OH)_4$ (µM)	CL	44±7	403±63	522±53	490±87	485±83	521±61	532±45	568±39	629±39	635±51	666±66	665±60	712±54	725±53
	HI	48±11	337±79	439±82	441±72	435±60	477±37	496±56	546±52	595±78	671±94	695±98	717±103	725±106	763±100
SO_4^{2-} (µM)	CL	21.9±0.6	21.4±0.5	21.2±0.7	20.9±0.6	20.7±0.7	20.3±0.6	19.9±0.5	19.3±0.6	18.7±0.4	18.6±0.5	18.4±0.5	18.6±0.5	18.6±0.5	18.6±0.5
	HI	21.8±0.5	21.7±0.4	21.6±0.6	21.3±0.5	21.1±0.6	20.6±0.5	20.2±0.4	19.5±0.6	18.7±0.6	18.5±0.7	18.3±0.7	18.4±0.8	18.4±0.9	18±0.8

Table S4: Fluxes of solutes (mmol m^{-2} d^{-1}) across the sediment-water interface calculated from lander data (BIGO) and porewater profiles (PW) at the control and high-impact sites. Positive fluxes are directed into the water column and vice versa. Also listed are the derived POC remineralization rates (mmol C m^{-2} d^{-1}).

Station	Chamber	Area	PO_4^{3-}	NO_3^-	NO_2^-	NH_4^+	$Si(OH)_4$	TOU	DIC	TA	$RPOC_{TOT}$
BIGO-I-1	K1	HI	0.02	-0.08	0.023	0.49	2.70	-8.52	12.20	1.23	8.13
	K2	HI	0.06	-0.23	0.030	1.34	3.30	-8.84	-	-	9.16
BIGO-I-2	K1	HI	-0.03	-0.22	0.034	1.04	3.29	-9.34	10.21	4.34	9.41
	K2	HI	0.03	-0.16	0.037	1.12	4.38	-9.06	12.75	5.60	9.13
BIGO-I-3	K1	HI	-0.01	-0.30	0.013	1.34	4.01	-7.80	8.68	6.35	8.30
	K2	HI	0.04	-0.35	0.008	1.56	3.49	-8.11	8.82	4.42	8.79
BIGO-I-4	K1	HI	0.05	-0.38	0.003	1.42	3.23	-6.70	8.76	6.94	7.45
	K2	HI	0.02	-0.30	0.012	1.51	3.19	-5.61	9.84	5.24	6.44
BIGO-I-5	K1	HI	0.03	-0.36	0.001	0.97	2.47	-3.12	8.64	9.45	3.89
	K2	HI	0.07	-0.41	0.005	1.78	3.10	-3.59	9.16	9.23	4.92
BIGO-I-6	K1	HI	0.04	-0.39	0.007	1.32	3.40	-5.40	6.04	0.77	6.22
	K2	HI	0.06	-0.37	0.019	1.50	3.92	-5.98	11.67	7.78	6.85
BIGO-II-1	K1	HI	0.01	-0.27	0.032	1.13	3.10	-11.81	14.03	3.14	11.75
	K2	HI	0.01	-0.17	0.038	1.10	2.93	-9.04	13.38	6.09	9.11
BIGO-II-2	K1	CL	0.04	-0.26	0.043	1.33	5.11	-9.69	14.31	8.05	9.98
	K2	CL	0.07	-0.35	0.052	1.36	4.23	-9.08	11.59	6.81	9.55
BIGO-II-3	K1	CL	0.37	-0.27	0.028	2.29	4.55	-10.55	21.06	15.60	11.42
	K2	CL	0.04	-0.25	0.020	1.56	3.95	-8.93	13.54	9.58	9.44
BIGO-II-4	K1	CL	0.22	-0.78	-0.111	4.63	5.00	-	25.01	14.66	
	K2	CL	0.06	-0.37	-0.002	1.82	3.60	-6.49	31.75	18.54	7.54
MUC5		HI	-	-	-	0.48	2.27	-	-	3.95	
MUC6		HI	-	-	-	0.64	2.45	-	-	5.18	
MUC9		HI	-	-	-	0.57	3.43	-	-	3.86	
MUC15		HI	-	-	-	0.26	0.73	-	-	0.73	
MUC21		HI	-	-	-	0.48	3.65	-	-	5.68	
MUC22		HI	-	-	-	1.27	4.22	-	-	6.42	
MUC28		HI	-	-	-	0.44	7.80	-	-	2.85	
MUC29		HI	-	-	-	1.39	7.28	-	-	13.69	
MUC33		HI	-	-	-	1.42	7.09	-	-	11.79	
MUC1		CL	-	-	-	1.23	7.05	-	-	8.45	
MUC2		CL	-	-	-	0.87	8.22	-	-	5.44	
MUC7		CL	-	-	-	1.54	7.44	-	-	11.04	
MUC12		CL	-	-	-	1.08	3.62	-	-	6.17	
MUC20		CL	-	-	-	2.40	8.78	-	-	9.68	
MUC23		CL	-	-	-	2.24	7.55	-	-	19.59	
MUC26		CL	-	-	-	0.95	4.19	-	-	4.93	
MUC31		CL	-	-	-	2.20	7.84	-	-	14.21	

Table S5: Pyrite concentrations (wt.%) in surface sediments (0–1 cm) at the study site.

Station	Area	Pyrite (wt.%)
MUC5	HI	0.44
MUC6	HI	0.45
MUC9	HI	0.23
MUC15	HI	0.79
MUC21	HI	0.34
MUC22	HI	0.37
MUC28	HI	0.52
MUC29	HI	0.55
MUC33	HI	0.29
MUC1	CL	0.34
MUC2	CL	0.40
MUC7	CL	0.46
MUC12	CL	0.45
MUC20	CL	0.39
MUC23	CL	0.52
MUC26	CL	0.43
MUC31	CL	0.60

Table S6. Modified differential equations of water column DIC and TA used in the coupled sediment-water column box model. For the original equations and parameter definitions, see Table S10 – S12 in Kalapurakkal et al., (2025). Modifications made here are in bold.

Parameter	Value	Unit
DIC - natural condition	$\frac{dDIC}{dt} = (-R_{POCP} + F_{benDIC}(t) - F_{exDIC}(t) - F_{CO2} + \mathbf{F_{benDICCa}}(t))/thwc$	mmol cm^{-3} yr^{-1}
DIC - resuspension	$\frac{dDIC}{dt} = (-R_{POCP} + (1 - traw) * (F_{benDIC}(t) + \mathbf{F_{benDICCad}}) + traw * (F_{benDICd}(t)+) + F_{exDIC}(t) - F_{CO2})/thwc$	mmol cm^{-3} yr^{-1}
TA - natural condition	$\frac{dTA}{dt} = (F_{benTA}(t) - F_{exTA}(t) + \mathbf{F_{benTACa}})/thwc$	mmol cm^{-3} yr^{-1}
TA - resuspension	$\frac{dTA}{dt} = ((1 - traw) * (F_{benTA}(t) + \mathbf{F_{benTAd}}) + traw * F_{benTAd}(t) + F_{exTA}(t))/thwc$	mmol cm^{-3} yr^{-1}

Where:

$\mathbf{F_{benTACa}} = \frac{9}{10000} \cdot 365$ mmol cm^{-2} yr^{-1}

$\mathbf{F_{benDICCa}} = 0.5 \cdot \mathbf{F_{benTACa}}$ mmol cm^{-2} yr^{-1}

$F_{benDICCad} = R_{POCox} + \mathbf{F_{benDICCa}} - \mathbf{freTA(t)} \cdot (\mathbf{\frac{9.2}{10000} \cdot 365})$

$\mathbf{F_{benTACad}} = -fre(t) * \left(r_{TApyox} * k_{PYox} * CPYd(t) * thtr - r_{TApy} * r_{Pypoc} * k_{Poca} * CPOCd(t) * (thsd - thtr)\right) + r_{TApy} * (1 - fre(t)) * r_{Pypoc} * k_{Poca} * CPOCd(t) * thsd + \mathbf{F_{benTACa}} - \mathbf{freTA(t)} \cdot (\mathbf{\frac{6.7}{10000} \cdot 365})$

freTA(t) defines the frequency and duration of each resuspension event (Kalapurakkal et al., 2025).

References

ICES: Manual for the Baltic International Trawl Surveys (BITS), https://doi.org/10.17895/ICES.PUB.2883, 2017.

Kalapurakkal, H. T., Dale, A. W., Schmidt, M., Taubner, H., Scholz, F., Spiegel, T., Fuhr, M., and Wallmann, K.: Sediment resuspension in muddy sediments enhances pyrite oxidation and carbon dioxide emissions in Kiel Bight, Commun Earth Environ, 6, 156, https://doi.org/10.1038/s43247-025-02132-4, 2025.